Biophysical Chemistry 205 (2015) 41–50

Contents lists available at ScienceDirect

Biophysical Chemistry

journal homepage: http://www.elsevier.com/locate/biophyschem

Chiral recognition of bilirubin and biliverdin in liposomes and micelles

Pavlína Novotná [a], František Králík [a], Marie Urbanová [b,*]

[a] Department of Analytical Chemistry, University of Chemistry and Technology, Prague, Technická 5, 166 28 Prague 6, Czech Republic
[b] Department of Physics and Measurements, University of Chemistry and Technology, Prague, Technická 5, 166 28 Prague 6, Czech Republic

HIGHLIGHTS

- We studied the interaction of bilirubin and biliverdin with model membranes.
- A differing interaction with liposomes and micelles was observed for the pigments.
- The different nature of the pigments influenced their penetration into the bilayer.
- In the presence of liposomes, bilirubin favorably interacted with serum albumin.
- The presence of surfactant completely changed biliverdin binding to the protein.

GRAPHICAL ABSTRACT

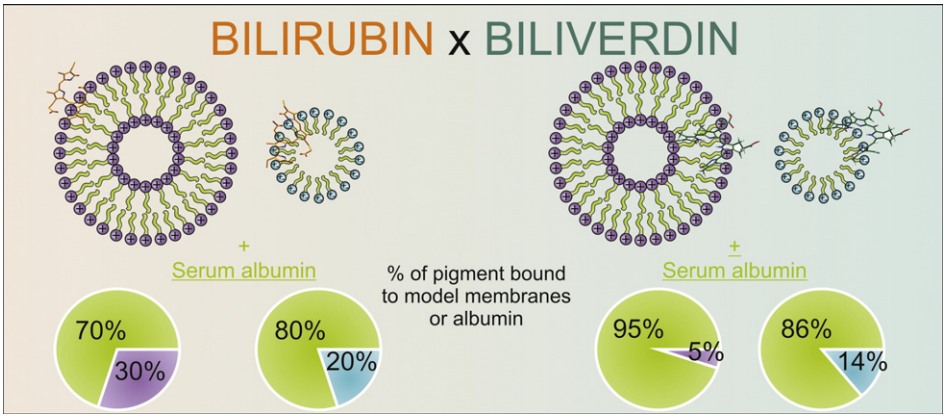

ARTICLE INFO

Article history:
Received 18 April 2015
Received in revised form 30 May 2015
Accepted 1 June 2015
Available online 4 June 2015

Keywords:
Electronic circular dichroism
Liposome
Micelle
Bilirubin
Biliverdin
Serum albumin

ABSTRACT

The structural formula of biologically important chiral pigments bilirubin and biliverdin differs only by one double bond. We showed that this results in dissimilar interactions with two models of membranes: cationic liposomes composed of 3β-[N-(N′,N′-dimethylaminoethane)-carbamoyl]cholesterol and zwitterionic micelles from 3-[(3-cholamidopropyl)dimethylammonio]-1-propanesulfonate (CHAPS). While the liposomes recognized the P-form of bilirubin, the micelles recognized its M-form. Both recognized the P-form of biliverdin.
Our study also comprised ternary systems consisting of the pigments, model membranes and serum albumin (human and bovine). Bilirubin preferentially interacted with the albumins even in the presence of the liposomes. On the other hand, biliverdin preferred the liposomes. Remarkably, the presence of CHAPS completely changed the biliverdin binding to the protein.
Because our study was oriented on different chiral interactions, a chiroptical method of electronic circular dichroism was chosen as the principal method to study our systems. As complementary methods, UV–vis absorption and fluorescence emission were used.

Abbreviations: BR, bilirubin; BV, biliverdin; BSA, bovine serum albumin; CHAPS, 3-[(3-cholamidopropyl)dimethylammonio]-1-propanesulfonate; CMC, critical micellar concentration; DC-cholesterol, 3β-[N-(N′,N′-dimethylaminoethane)-carbamoyl]cholesterol hydrochloride; DMPC, 1,2-dimyristoyl-*sn*-glycero-3-phosphocholine; ECD, electronic circular dichroism; HSA, human serum albumin; IR, infrared; UV–vis, ultraviolet–visible.

* Corresponding author at: Department of Physics and Measurements, Institute of Chemical Technology, Prague, Technická 5, 166 28 Prague 6, Czech Republic.
E-mail address: Marie.Urbanova@vscht.cz (M. Urbanová).

http://dx.doi.org/10.1016/j.bpc.2015.06.001
0301-4622/

1. Introduction

Our study is focused on two naturally occurring bile pigments: yellow-orange bilirubin (BR) and green-blue biliverdin (BV). BV is formed as a result of an oxidative breakdown of the heme moiety of hemoglobin and is usually immediately reduced to free BR. However, it can be for instance seen as a cause of a green color in bruises. On the other hand, BR is standardly occurring in low concentrations in blood plasma. Both of the pigments may be found in an excess in the blood during the hepatic diseases like jaundice [1,2].

BR and BV are linear tetrapyrroles and their structural formula differs only by one double bond localized in the central part of the BV molecule (Fig. 1). However, their spatial structure differs substantially [3–6]. In solution, BR is normally stabilized by six intramolecular hydrogen bonds while the double bond in BV restricts its possible conformations and, hence, there are only two intramolecular hydrogen bonds in BV. The spatial structure gives rise to two enantiomeric forms of both bile pigments: the P- and M-helical forms (Fig. 1). The racemization barrier between the two enantiomers is, nevertheless, very low and therefore we always get a racemate in a solution without a chiral selecting agent.

In the presence of a chiral selector, BR and BV often preferably interact only in one of their enantiomeric forms forming one diastereoisomeric complex with the selector [7–16]. Selectors of different chemical natures have been used previously and described in the literature: proteins and peptides [7,10,11,17–21], cyclodextrins [8,13–16], metals [9], alkaloids [22] and guanosine assemblies [23] among others. A considerable part of the studies [21,24–29] is devoted to BR interactions with different models of membranes — either liposomal or micellar. These studies were inspired partly by a search for a good chiral selector of BR, also by describing the chiral properties of the models and last but not the least by the biological effects of increased BR concentrations. The studies proved the enantioselective interaction of BR with models of membranes — either the P- or M-form of BR was preferentially recognized by the membranes. The enantioselective attack of BR on the nerve cells is one of the most debated negative effects of this pigment in our organism. Therefore different models of membranes were previously studied to explain these properties of BR.

Our work focuses on two non-standard models of membranes and their interaction with both BR and BV. We studied cationic liposomes composed of chiral 3β-[N-(N′,N′-dimethylaminoethane)-carbamoyl]cholesterol (DC-cholesterol, structure in Fig. 2). The interaction of bile pigments with positively charged model membranes has been scarcely studied before for BR [30] and never for BV. Interestingly, the BV interactions with model membranes or with cellular membranes have not been described at all. We have chosen this specific model because of its charge and also because the main functional unit in its structure is very close to cholesterol. Previously, we have studied [21] BR interactions with different zwitterionic and negatively charged liposomes and also with their mixtures with cholesterol, but we did not observe any specific interaction with cholesterol. Our unpublished results also showed that BV did not interact enantioselectively with classical membrane models from zwitterionic 1,2-dimyristoyl-*sn*-glycero-3-phosphocholine (DMPC), 1,2-dioleoyl-*sn*-glycero-3-phosphocholine and sphingomyelin to negatively charged 1,2-dimyristoyl-*sn*-glycero-3-phosphocholine liposomes.

The newly used cationic model should simulate the positively charged parts of cellular membrane surfaces. However, the DC-cholesterol liposomes could also serve as an interesting chiral selecting agent for both pigments if the liposomes were to interact only with one of the enantiomeric forms of the pigments.

As a comparative model, micelles from zwitterionic 3-[(3-cholamidopropyl)dimethylammonio]-1-propanesulfonate (CHAPS, structure in Fig. 2) were chosen. This compound also has a functional group consisting of several cycles, in this case of an aliphatic nature. We suppose that these micelles can be used as a good and relatively simple selector for the enantioselective recognition of BR and BV.

Our study also includes ternary systems consisting of bile pigments, model membranes and serum albumin. We included serum albumin in our study because BR and BV are both known to bind to this protein enantioselectively [7,11,17–20] and this interaction is vital as serum albumin works as the main transporter of BR in the blood circulation [31] and it plays an important role during the BR and BV oxidative cycles [31]. We primarily chose human serum albumin (HSA) as studies with this protein are of human health importance. HSA has three binding sites with P-selectivity of BR: one primary site with a considerably high binding constant ($K_a \sim 10^8\ M^{-1}$) and two secondary sites with lower and similar binding constants ($K_a \sim 10^6\ M^{-1}$) [18–20,32–34]. HSA has also at least two binding sites for BV with the M-stereoselectivity [35–37]. Therefore, it is interesting to follow such ternary systems, especially to clarify whether bile pigments would prefer to bind to HSA or to the model membranes establishing their potential toxicity towards cell membranes with a positive charge.

As a comparative protein, especially for the study with BR, bovine serum albumin (BSA) was chosen. BSA has an opposite stereoselectivity of the bilirubin primary binding site as compared with HSA but the two secondary binding sites also have P-stereoselectivity [7,17]. However, it has an M-stereoselectivity for BV similar to that of HSA and, moreover,

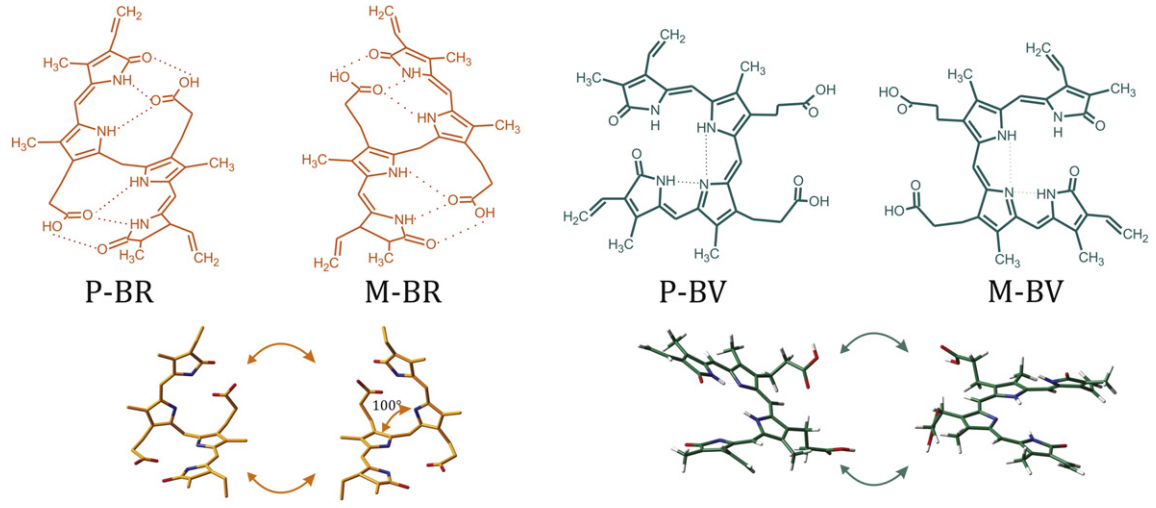

Fig. 1. The structural formulas of the enantiomeric P- and M-helical forms of BR and BV and their spatial chiral structures, denoted as P-BR, M-BR and P-BV, M-BV. The hydrogen bonds are shown as dotted lines.

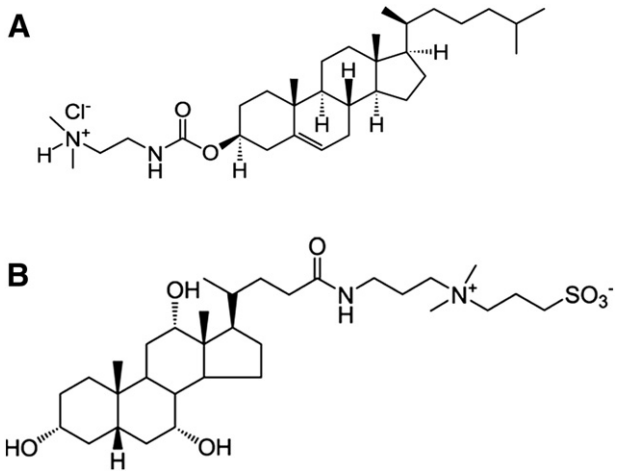

Fig. 2. The structural formula of (A) 3β-[N-(N′,N′-dimethylaminoethane)-carbamoyl]cholesterol hydrochloride (DC-cholesterol) and of (B) 3-[(3-cholamidopropyl)dimethylammonio]-1-propanesulfonate (CHAPS).

the selected proteins have high homology [31] and, hence, the results gained from the studies of such complex systems with model membranes can be verified and compared by using both HSA and BSA. Since the results from the BSA study were used only as comparative materials to the study with HSA, they are included in Supplementary material, Chapter 1.

As our study was particularly concerned with different chiral forms of BR and BV which are preferentially recognized by model membranes or serum albumins, we chose the chiroptical method of electronic circular dichroism (ECD) as the primary method to study our systems. This spectroscopy is sensitive to BR and BV enantiomeric excess [7–9,17,21,23]. As complementary methods, absorption spectroscopy in the ultraviolet and visible (UV–vis) region and fluorescence emission spectroscopy were used.

2. Material and methods

2.1. Materials

The 3β-[N-(N′,N′-dimethylaminoethane)-carbamoyl]cholesterol hydrochloride (DC-cholesterol, structure in Fig. 2), 1,2-dimyristoyl-*sn*-glycero-3-phosphocholine (DMPC) and sphingomyelin lipids and the 3-[(3-cholamidopropyl)dimethylammonio]-1-propanesulfonate (CHAPS, structure in Fig. 2) surfactant were purchased from Avanti Polar Lipids (Alabaster, AL). The bilirubin-IXa (BR) and biliverdin hydrochloride (BV) were purchased from Frontier Scientific (USA). The human serum albumin (A3782) and bovine serum albumin (A7030) were purchased from Sigma Aldrich. All of the chemicals were used without further purification.

2.2. Preparation of large unilamellar vesicles

The liposomes were prepared using the standard procedures [38] and the specifics of their preparation were described in our previous publication [21,39]. The final lipid concentration in the prepared liposomal solution was calculated based on the weight of the dried lipid [40–44]. The dynamic light scattering method confirmed the narrow size distribution of the vesicles with the maximum at 111 ± 2 nm.

For the testing of the scattering effects, larger liposomes 216 ± 10 and 420 ± 14 nm were prepared by extrusion and smaller liposomes 82 ± 8, 51 ± 8 and 39 ± 8 nm were prepared by sonication.

2.3. Sample preparation

The solution of a BR or BV sodium salt (concentration 0.005 M) was prepared to achieve a higher solubility of the bile pigment [8]. Powdered BR was dissolved in a 3:1 molar excess of a sodium hydroxide aqueous solution so that a complete neutralization was achieved and the solution was centrifuged to confirm the complete dissolution of BR. A 2:1 molar excess of sodium hydroxide was used for the BV solutions.

These solutions were used as stock solutions but for no longer than 2 h for BR and one day for BV. During that time, the solutions were stored in the dark and in a refrigerator. The solution of the CHAPS micelles was prepared by dissolving the appropriate amount of weighed CHAPS in the phosphate buffer to achieve a 16×10^{-2} M bulk solution. All the spectral measurements were conducted in solutions of a 1×10^{-2} M phosphate buffer (pH = 7.4). In the systems with serum albumin, the solution of BR with the liposomes or micelles was prepared first and then the stock solution of serum albumin (concentration 1×10^{-3} M) was added.

For the ECD measurements, the BR concentration was in the range of 1×10^{-5}–5×10^{-5} M. The concentration of DC-cholesterol was 1×10^{-3} M and of CHAPS was 8×10^{-3} M or 2×10^{-3} M. The concentration of serum albumin was 1×10^{-5} M. For the measurement of fluorescence emission spectra, the concentration of BR was 1×10^{-5} M, of serum albumin 1×10^{-5} M (1:1 BR:HSA ratio) and the concentration of DC-cholesterol was 1×10^{-3} M and that of CHAPS was 8×10^{-3} M.

None of the measured solutions showed any presence of aggregates or precipitates as was confirmed by their centrifugation.

2.4. Electronic circular dichroism and UV–vis absorption

The ECD and UV–vis absorption spectra were measured in a quartz cuvette with an optical path length of 1 cm or 1 mm (Hellma, Germany) using a J-810 spectrometer (Jasco, Japan). The conditions of the measurements were as follows for the region of 250–800 nm: a scanning speed of 100 nm/min, a response time of 1 s, a resolution of 1 nm, a bandwidth of 1 nm and a sensitivity of 100 mdeg; for the region of protein absorption (200–300 nm): a scanning speed of 10 nm/min, a response time of 8 s, a resolution of 1 nm, a bandwidth of 1 nm and a sensitivity of 100 mdeg. The final spectrum was obtained as an average of 5 accumulations in all cases. The spectra were corrected for a baseline by subtracting the spectra of the corresponding buffer. The ECD measurements were conducted at room temperature (25 °C).

Spectra are presented in molar circular dichroism units relative to the concentration of BR or BV. Liposomes of different sizes were tested (Section 2.2) to find whether there is a spectral distortion in the ECD spectra caused by scattering from the particles. No size-related effects were observed for the tested liposomes up to 111 nm. The 111 nm liposomes were consequently used in all the measurements because of their narrow size distribution due to extrusion. For the 216 ± 10 and 420 ± 14 nm liposomes, high spectral noise accompanied with a smaller distortion of the ECD bands was observed suggesting scattering effects.

The ECD spectra in the region of protein absorption were further analyzed with the CDNN software [45] to determine the content of different secondary structures in the protein structure (Table S1). Further details can be found in Supplementary materials (Table S2). The UV–vis absorption spectral envelope was further analyzed and separated into spectral components. Further details can be found in Supplementary materials (Table S2).

2.5. Fluorescence emission spectroscopy

The fluorescence emission spectra were measured on a J-810 spectrometer equipped with a fluorescence accessory FDCD-404L (Jasco, Japan). The spectra were measured in a quartz cuvette with an optical path length of 1 cm (Hellma, Germany). The conditions of the

BR measurements were as follows: a spectral region of 450–800 nm, an excitation wavelength of 430 nm, a response time of 2 s, a resolution of 1 nm, a bandwidth of 10 nm and a sensitivity of 1000 V. The conditions of the BV measurements were as follows: a spectral region of 390–650 nm, an excitation wavelength of 380 nm, a response time of 2 s, a resolution of 1 nm, a bandwidth of 10 nm and a sensitivity of 900 V. The final spectrum was obtained as an average of 5 accumulations in both cases. All the measurements were conducted at 25 °C. The spectra were corrected for the inner filter effect according to ref. [46].

To rule out dimerization or aggregation of the components, a concentration range for all the measured compounds was determined, where the emitted intensity depended in a linear way on the concentration.

The fluorescence emission spectral envelope was further analyzed and separated into spectral components. Further details can be found in Supplementary materials (Table S3).

3. Results and discussion

Although the spatial structure of BR and BV is not planar (Fig. 1), the compounds did not have any ECD signal in the phosphate buffer solution (Figs. 3 and 6). This was observed due to the well-known fact that, in an isotropic media, both pigments form a racemate of two enantiomeric helical forms: P and M which results into a zero optical activity of the whole solution.

Therefore, to enable the study of these pigments with chiroptical techniques, a chiral matrix that recognizes only one of the enantiomers is necessary. Various but unfortunately not numerous examples of these can be found in the literature. The liposomes composed of chiral lipids and micelles composed of chiral surfactants certainly do not represent a simple model of chiral matrix. However, the biological relevance of this model is important. Moreover, the studies of bile pigment competition between binding to the liposomal selectors and serum albumin are interesting from the biochemical point of view because they may approximate the situation in living organisms. Hence, we studied the BR and BV solutions with chiral DC-cholesterol liposomes and CHAPS micelles to discover whether the pigments will be enantioselected by these model membranes.

3.1. Bilirubin interaction with the DC-cholesterol liposomes and CHAPS micelles

Fig. 3 depicts the ECD and UV–vis absorption spectra of BR with the DC-cholesterol liposomes and with the CHAPS micelles. The observed non-zero ECD signal indicated that both the DC-cholesterol liposomes and the CHAPS micelles preferentially bound one of the BR enantiomers.

In the ECD spectrum of BR with the DC-cholesterol liposomes, a negative couplet was observed localized at 416(+)/472(−) nm. A negative BR couplet was previously assigned to the M-form of BR [37]. In the UV–vis absorption spectra of BR alone (Fig. 3), a band localized at 438 nm was observed. This band is in fact an overlap of two electronic transitions (~430 and ~470 nm) which come from the two similar chromophores in the BR structure [47] (Fig. 1). In the UV–vis absorption spectra of BR with the DC-cholesterol liposomes, the BR spectral band was superposed by the increased background absorption and scattering which came from the liposomes. However, the spectra still clearly showed that the central band was diversified and, hence, the intensity of the two bands at 422 and 471 nm was not same. The intensity of the band localized at lower wavelengths (the higher energy transition) was higher. These observations imply that the chromophores were influenced differently by the interaction with the liposomes. As the intensity of the higher energy transition increases with a more closed BR conformation, which is high in energy (~25 kcal/mol above the global energy minimum conformation), it is possible that the interaction with the liposomes caused BR to assume a conformation which is not strictly the same as the conformation it takes in the solution and that the torsion angle in its structure would be smaller.

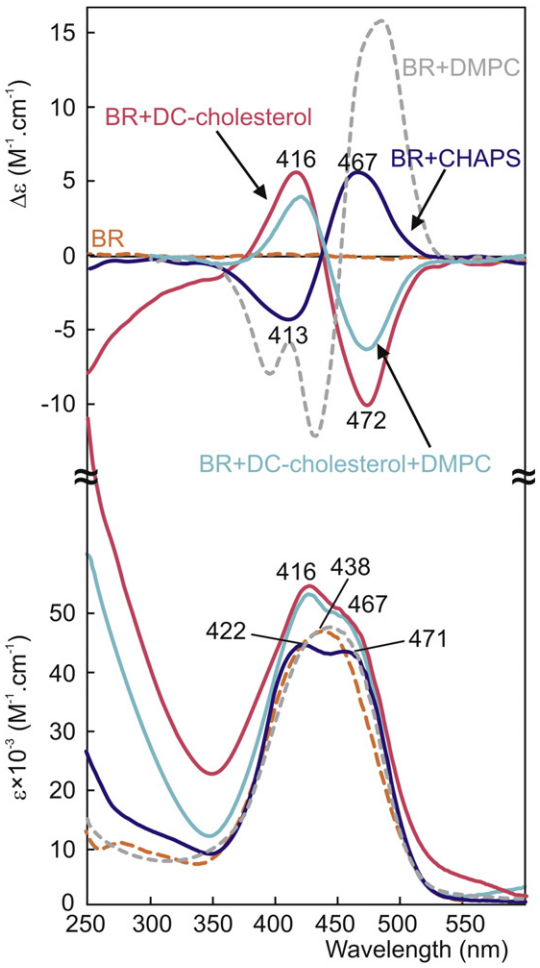

Fig. 3. The ECD (top) and UV–vis absorption (bottom) spectra of BR alone in the solution and in the presence of the DC-cholesterol liposomes and the CHAPS micelles. It also depicts the BR spectra with the DMPC liposomes and with the liposomes from the DC-cholesterol/DMPC mixture. The concentration of BR was 1×10^{-5} M, that of the lipid was 1×10^{-3} M and that of CHAPS was 8×10^{-3} M.

The DC-cholesterol liposomes have a positive charge on their surface, while BR can have up to two negative charges in its structure depending on pH. At a pH of 7.4, which we used [48–50], both carboxylic groups in the structure of BR are dissociated. Hence, we suppose that the observed interaction is of an electrostatic nature. A study with the liposomes composed of DC-cholesterol mixed in a 1:1 molar ratio with zwitterionic DMPC (Fig. 3) was performed to clarify this statement. In such liposomes, the lipids are not evenly distributed but form domains composed of only one lipid. Because of this, BR could interact either with the DC-cholesterol domain by the supposed electrostatic mechanism, which is very strong, or with the DMPC domain by the hydrophobic mechanism. Although BR interacts in its P-form with the DMPC liposomes (Fig. 3), a negative couplet was again observed in the spectra (Fig. 3), which means that the M-form of BR interacted. This showed that the interaction with the DC-cholesterol liposomes is based on stronger forces than merely hydrophobic and confirmed the electrostatic nature of the interaction. Also at increased concentrations (10^{-1} M of DC-cholesterol and 7×10^{-2} M of BR), BR aggregated with the DC-cholesterol liposomes, which did not happen with the DMPC or other zwitterionic liposomes.

Fig. 4 shows the fluorescence spectra of BR with different chiral agents. A very intense fluorescence quenching did not allow measurement of the fluorescence spectra of BR alone in the phosphate buffer.

Because of that, a spectrum of BR bound to the primary binding site of HSA is used as a reference. The maximum of the spectrum of BR with the DC-cholesterol liposomes was red shifted in comparison with the reference spectrum. This indicates that BR was situated in a more polar environment, which is localized near the surface, when interacting with the DC-cholesterol liposomes. This also implies that it is highly improbable that BR penetrated into the DC-cholesterol bilayer. The position of the spectral maxima was also similar to BR interacting with the sphingomyelin liposomes, for which the penetration of BR inside to the bilayer was not observed.

In the ECD spectrum of BR with the CHAPS micelles (Fig. 3), a positive couplet localized at 413(−)/467(+) nm was observed. This couplet was assigned to the P-form of BR. The BR band in the UV–vis absorption spectra was quite diversified as well but the two bands at 416 and 467 nm were almost equal in intensity. The position of the maximum in the fluorescence emission spectrum (Fig. 4) was between the maxima of the BR with HSA spectrum and of the BR with the DC-cholesterol liposomes spectrum.

The CHAPS micelles are zwitterionic. Due to their chemical composition, the polarity of the environment in the inner layer of the CHAPS micelles should not be so different from the bilayer of the DC-cholesterol liposomes. Nevertheless, we observed that BR interacted with them in the P-form and was localized in the less polar region, hence more inside the hydrophobic inner region, as compared with the DC-cholesterol liposomes. The nature of the interaction was probably hydrophobic and we believe that this is the reason for the pigment penetration into the hydrophobic region. On the other hand, in the system with the DC-cholesterol liposomes, the electrostatic interactions were probably quite strong and accordingly the hydrophobic interactions were overruled and BR did not participate in them. As a consequence, the fluorescence spectra showed that BR did not penetrate further into the bilayer. This was confirmed by the UV–vis spectra, where the diversification of the BR absorption band showed that one of the chromophores is more influenced by the interaction, while the second one probably remains more exposed to the solution.

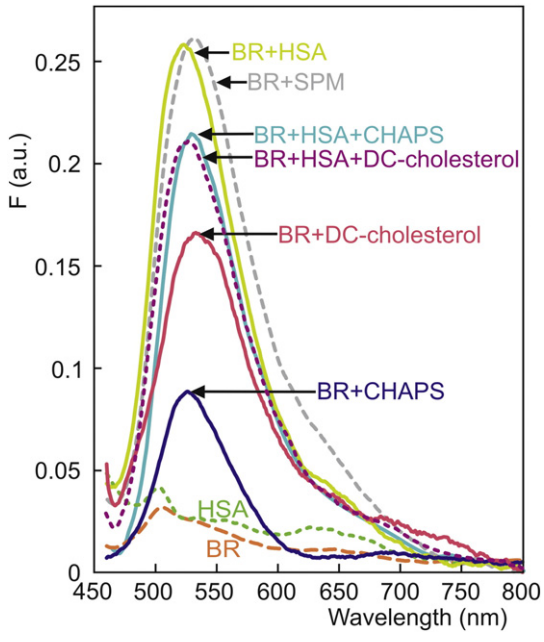

Fig. 4. The fluorescence emission spectra of BR and HSA alone in the solution of a phosphate buffer and of BR in the presence of HSA, the DC-cholesterol liposomes, and the CHAPS micelles and in the ternary systems with HSA and the DC-cholesterol liposomes or the CHAPS micelles. The spectrum of BR with the sphingomyelin liposomes is also shown. The concentration of BR and HSA was 1×10^{-5} M, of the lipid was 1×10^{-3} M and of the CHAPS surfactant was 8×10^{-3} M.

Hence, we found out that both the DC-cholesterol liposomes and the CHAPS micelles are appropriate chiral matrices that preferentially bind one of the BR enantiomers with the participation of different interaction forces. The results also stress that chirality plays an important role in the BR interactions in the human organism. With respect to the chosen model membranes, different chiral forms of BR can be selected. The membrane chiral selectors of BR are potentially interesting not only due to their enantiorecognitive properties, but also because of the biological aspect of BR binding to the membranes in living organisms which is undesirable as it often leads to cell apoptosis. Our results indicated that BR was prone to binding to positively charged parts of cell membranes with stronger forces than to the zwitterionic parts. Moreover, the cholesterol-like character of the membrane components was not an obstacle as was shown both with the DC-cholesterol and CHAPS models. However, only a small amount of BR was found unbound in the human organism [31]. It is mostly found bound to the blood carrier proteins or lipoid particles and eventually is glucoronated to be transferred and excluded from the body. Therefore, the possibility of the binding needs to be studied further in more complex systems where the concurrence of membranes with the traditional BR binding partners is studied. Such a study is carried out in the next section with the most common BR binding protein in blood circulation.

3.2. Competition between the membrane selectors and human serum albumin in terms of bilirubin interaction

In this part, we included HSA in the study of BR interactions with model membranes. HSA is known to bind BR with a very high binding constant ($K_a \sim 10^8$ M^{-1}) [31] as its main transporter in the human organism. This study could clarify whether BR would bind to HSA or to the positively charged domains of cellular membranes which could result in undesirable negative effects of this pigment.

Although numerous studies of BR and BV binding to serum albumin [7,17–20] have already been published, it was previously found to be very specific and strongly dependent on the ambient conditions, especially on the pH but also on ionic strength and other conditions in the solution. Therefore, Fig. 5 depicts the ECD spectra of BR with HSA for the BR:HSA ratios from 1:1 to 5:1 measured under the conditions that we used in the whole work and that were described in the Materials and methods section. A similar study was also carried out with BSA and is described in detail in Supplementary material, Chapter 1, Figs. S1 and S2.

HSA had no signal in the region typical of BR absorption. Besides this region, a region typical of the aromatic amino acids was studied as it reflects the spatial structure of the protein (Fig. 5). A region where the secondary structure of the peptides is reflected was studied as well. The spectra are not shown here but the detailed results of the analysis of the secondary structure changes based on these spectra can be found in Chapter 2 of Supplementary material (Table S1).

The measured spectral series for the binary system of BR with HSA showed that in the presence of serum albumin, BR had a non-zero ECD signal. A positive couplet was observed and its intensity was very similar up to a 3:1 ratio of BR:HSA. No significant changes were observed in the region where the spatial structure of HSA is reflected. In the UV–vis absorption spectral series, the maximum of the BR central band (originally at 438 nm) shifted to the higher wavelength 454 nm for the 1:1 to 3:1 ratios and then moved back to lower wavelengths. These observations both from the ECD and UV–vis spectra confirm three BR binding sites in the HSA structure which were described previously [18–20,32–34]. All of them preferentially bind the P-form of BR as can be concluded from the ECD spectra.

Fig. 5 also depicts the ECD spectra of BR with the DC-cholesterol liposomes in the presence of HSA. A spectral pattern consisting of three bands at 397(−)/447(+)/492(−) nm was observed. We interpret this pattern as a result of an overlap of two couplets, one from BR bound mainly to the primary site of HSA and a small one

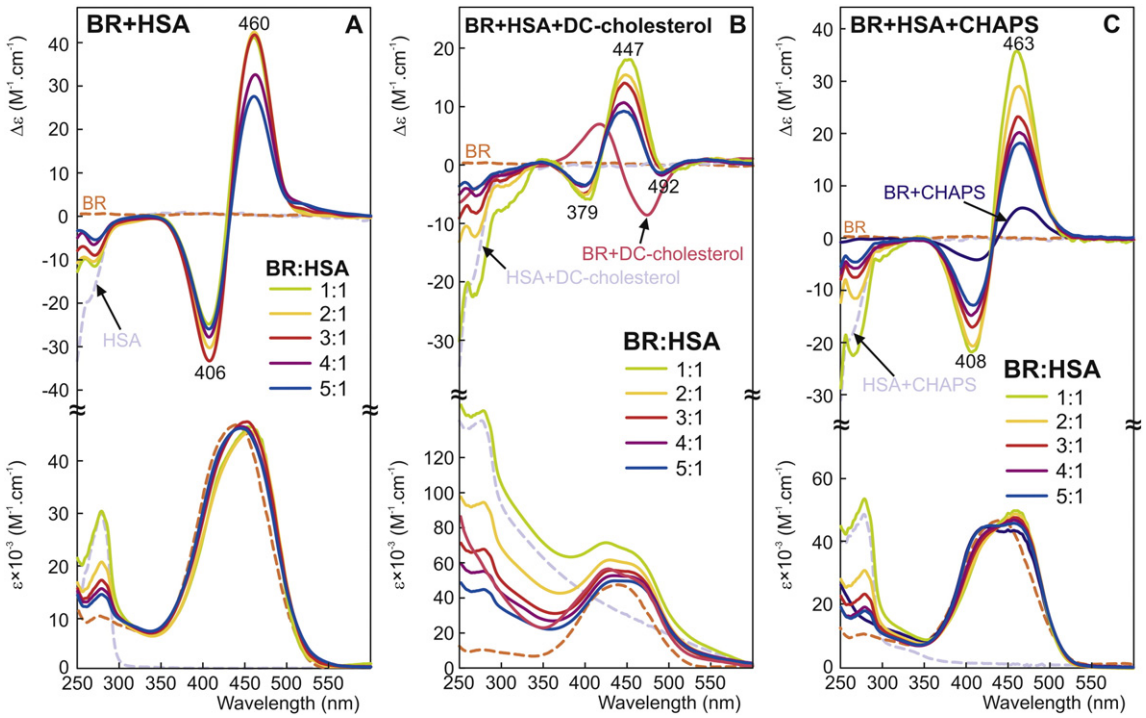

Fig. 5. A: The ECD (top) and UV–vis absorption spectra (bottom) of BR with HSA measured for the BR:HSA ratio from 1:1 to 5:1. The ECD spectra of HSA and BR are also shown. B: The ECD (top) and UV–vis absorption spectra (bottom) of BR with HSA in the presence of the DC-cholesterol liposomes measured for the BR:HSA ratios from 1:1 to 5:1. The ECD spectra of HSA with the DC-cholesterol liposomes, of BR and of BR with the DC-cholesterol liposomes are also shown. C: The ECD (top) and UV–vis absorption spectra (bottom) of BR with HSA in the presence of the CHAPS micelles measured for the BR:HSA ratios from 1:1 to 5:1. The ECD spectra of HSA with the CHAPS micelles, of BR and of BR with the CHAPS micelles are also shown. The concentration of HSA was 1×10^{-5} M, that of the lipid was 1×10^{-3} M, that of the CHAPS was 8×10^{-3} M and that of BR was given by the BR:HSA ratio and was in the region of 1×10^{-5} M–5×10^{-5} M.

from BR bound to the DC-cholesterol liposomes. This implies that even in the presence of the DC-cholesterol liposomes, BR still preferentially bound to HSA. The BR–HSA binding was, however, influenced by the liposomes. For the 1:1 ratio, the intensity of the band at 492 nm was almost negligible and also the intensity of the positive part of the couplet decreased to ~45% and of the negative part of the couplet decreased to ~25% of the original intensity measured in the solution without liposomes (Fig. 5). We have separated the UV–vis absorption spectra (Fig. 5) and the fluorescence emission spectra (Fig. 4) into the individual components and analyzed the BR binding in detail. While the results of interest are shown here, the in-depth specific information is included in Supplementary material, Tables S2 and S3). The analysis of the UV–vis absorption spectra from Fig. 5 showed that for the 1:1 ratio, the amount of unbound BR was negligible and 69% of bound BR was bound to HSA and 31% to the liposomes (65 and 35%, respectively, according to the analysis of the fluorescence spectra). Hence, the DC-cholesterol liposomes influenced the BR binding even to the primary binding site of HSA, to which BR has a very high binding constant.

The ECD intensities were also lower for the higher ratios. So, the spectra also show competition between the secondary binding sites and the liposomes. As for the higher ratios, the appearance of the negative band at 492 nm testified to BR binding to the liposomes to which BR binds with opposite chirality than that with which it binds to HSA. The different and considerably lower extinction coefficient of BR bound to the liposomes (Fig. 3) than to HSA (Fig. 5) should be noted here. Hence, although the signal of BR bound to HSA seems more intense than that of BR bound to the liposomes, it does not signify that more BR is bound to the secondary binding sites of HSA than to the liposomes. The analysis of the UV–vis absorption spectra (Table S2) showed that for the 3:1 ratio 36% of bound BR was bound to the primary binding site of HSA, only 6% to the secondary sites and 58% to the DC-cholesterol liposomes. For the 5:1 ratio, it was 26% of BR bound to the primary site and 11% to the secondary sites of HSA and 63% to the liposomes. Hence, BR almost did not bind to the secondary sites of serum albumin and competitive binding to the primary site of HSA and to the liposomes occurred.

Minor spectral changes were observed in the ECD spectra in the region of the HSA absorption and implied the DC-cholesterol influence on HSA reflecting that DC-cholesterol hampered the BR binding to the secondary sites. The solutions had to be prepared very carefully; otherwise HSA formed aggregates with the liposomes. This confirmed their interaction which could have occurred also in the solutions where no aggregation took place. This probably influenced the spatial structure of the protein which was reflected in the spectra. However, its secondary structure was not meaningfully influenced.

A similar study carried out with comparative protein BSA (Supplementary material, Chapter 1.1, Fig. S1, Tables S2 and 3) provided similar results and conclusions. The BSA primary binding site binds an opposite enantiomer of BR than HSA does [7,17]. Therefore, studies with BSA were previously [8,17] used to verify and confirm the results obtained with HSA. Moreover, unlike HSA, BSA has a different stereoselectivity of the primary and secondary binding sites which makes the observations of the competition between the different sites and the liposomes more demonstrable.

Fig. 5C depicts the BR binding to the CHAPS micelles in the presence of HSA. A positive couplet was observed for all BR:HSA ratios suggesting the binding of the P-form of BR. The observed intensity even for the 1:1 ratio almost reached the intensity observed for the binary system of BR with HSA. A small part of BR bound to the micelles as well and this binding competed the binding to HSA. The analysis of the fluorescence spectra (the 1:1 BR:HSA ratio, Table S3) showed that 21% of BR was bound to the CHAPS micelles and 79% to HSA. For the higher ratios, the analysis of the UV–vis absorption spectra showed, that the binding to the CHAPS micelles was preferred over the binding to the HSA secondary binding sites (Table S2, e.g. for the 3:1 ratio 31% of bound BR bound to the primary site of HSA, 31% to the secondary sites and 38% to the micelles).

Comparable results were also obtained in the study with BSA (details and figures in Supplementary material, Chapter 1.1, Fig. S1, Tables S2 and 3). A preferential binding of BR to both the primary and secondary sites of BSA than to the CHAPS micelles was observed similarly to the HSA system. The negative couplet for BR bound to the primary site of BSA was overlapped by the positive couplet for BR bound to the CHAPS micelles. This could not be observed in the system with HSA because the couplets had a same sign.

The small amount of BR molecules interacting with the CHAPS micelles in the presence of HSA in comparison with other zwitterionic models we had used previously [51] might be caused merely by its functional unit similar to non-interacting cholesterol and also by the mono-layer character of this model.

The obtained results indicated that BR still preferentially interacts with the primary site of HSA even in the presence of positively charged membranes from DC-cholesterol although it is negatively charged under the conditions that occur in blood. This is quite the opposite to what had been previously observed with zwitterionic liposomic models of classical and neural cell membranes [51]. However, it confirmed our observations with cholesterol [21] as we did not observe any BR interaction with the liposomes which were partially composed of cholesterol. This means that when BR is transported in the blood by serum albumin it should not bind to positively charged membranes and should remain bound to the protein. In the case of pathologic states connected with increased amounts of BR when all the primary binding sites of HSA are occupied, the concurrence between the HSA secondary binding sites and positively charged membranes would occur and would result into partial BR binding to the positively charged membranes. On the other hand, the zwitterionic cholesterol-like micelles did not significantly bind BR even for higher ratios of BR:HSA.

3.3. Biliverdin interaction with the DC-cholesterol liposomes and CHAPS micelles in the presence of HSA

BV is a BR precursor on its degradation pathway. As the degradation is considerably fast [31], BV concentrations are usually not very high in the human organism. However, BV is also produced during BR oxidation cycle. Therefore, it is important to investigate its interactions with model membranes.

In the ECD spectrum of BV with the DC-cholesterol liposomes (Fig. 6), a positive band localized at 666 nm and a negative band at 390 nm were observed. These signs of spectral bands are typical of the P-form of BV. This implies that an enantioselective interaction between BV and the DC-cholesterol liposomes has occurred and that the P-form of BV has preferentially interacted with the DC-cholesterol liposomes.

The absorption bands in the UV–vis spectrum of BV solution were localized at: 672 nm (π–π^* transition in the C═C and C═N system of BV), 373 nm (π–π^* transition S_0 to S_2 of the delocalized π-system) and 316 nm (band typical for non-restricted open-chain bilatriens in a helical conformation) [47]. After the interaction with the DC-cholesterol liposomes, the bands shifted to 668, 385 and 332 nm and their relative intensity changed as well. The intensity of the band at lower wavelengths decreased and the intensity of the band at higher wavelengths increased. The absorption band at 668 nm is strongly associated with the spatial structure of BV and it reflects the size of the torsion angle between the two dipyrrinon units of BV. The changes in the relative intensity of the UV–vis absorption bands suggest that the torsion angle changed after the addition of the DC-cholesterol liposomes. These results are in accordance with the ECD results where the BV/DC-cholesterol interaction was indicated.

Similarly to BR, depending on pH, BV can have up to two negative charges in its structure [48–50] and at a pH of 7.4, which we used, it should be fully dissociated. Hence, its interaction with the positively charged liposomes is again most likely of an electrostatic nature.

In the presence of the DC-cholesterol liposomes, the BV florescence spectrum (Fig. 7) was shifted to a lower wavelength and was very

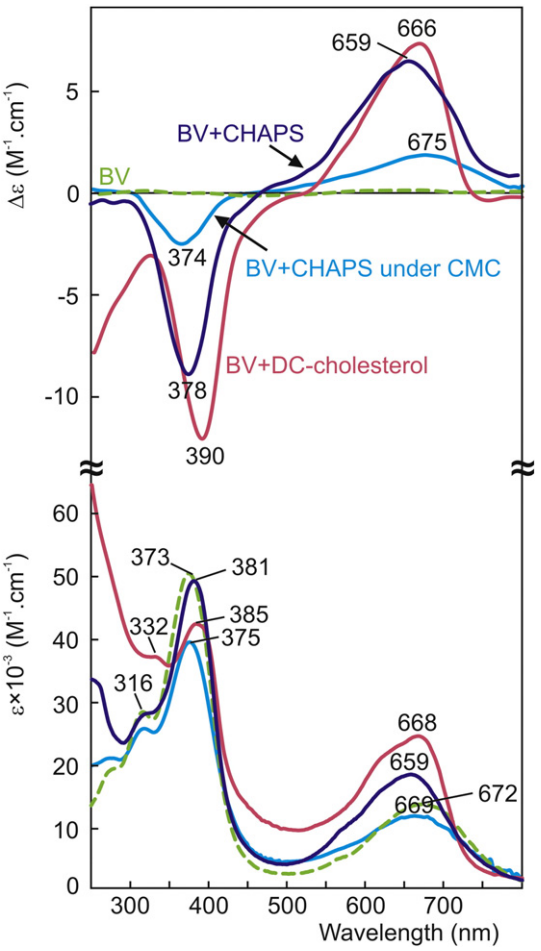

Fig. 6. The ECD and UV–vis absorption spectra of BV alone in the solution and in the presence of the DC-cholesterol liposomes and the CHAPS micelles both at CHAPS concentrations above and under CMC. The concentration of BV was 1×10^{-5} M, that of the lipid was 1×10^{-3} M and that of CHAPS was 8×10^{-3} and 2×10^{-3} M.

similar to the spectrum of BV with HSA. This shift implies that BV penetrated more into the non-polar environment of the bilayer than BR. So, this indicated that the hydrophobic interactions and maybe also other weak interactions supported by the double bond in the BV structure had played an important role.

The interaction with the CHAPS solution (Fig. 6) was studied at two different concentrations of CHAPS — below and above the CMC (6×10^{-3} M), and different results were obtained. The ECD spectra had the same signs for both concentrations of CHAPS. A positive band was observed at higher wavelengths (659 nm for the micellar solution and 675 nm for the solution with the unordered surfactant) and a negative band was observed at lower wavelengths (378 nm for the micellar solution and 374 nm for the unordered surfactant). In the UV–vis absorption spectra, bands at 659 and 381 nm were observed for the solution with the micelles. Bands at 669 and 375 nm were observed for the solution with the unordered surfactant. In the fluorescence spectra (Fig. 7), the band for BV bound to the CHAPS micelles was shifted to higher wavelengths as compared with BV bound to HSA.

The obtained results imply that BV interacted with the CHAPS surfactant and also with the micelles composed of this surfactant. In both cases, the ECD spectral envelope was a typical reflection of the P-form of BV which we, therefore, suppose preferentially interacted. However, in our opinion, the interaction with the micelles and unordered CHAPS must be of a different nature, as the position of the spectral bands was different and also because it did not change for different CHAPS concentrations above CMC. Although the conformation of BV remains the same in both cases, it is probable that with the micelles, the interaction occurs

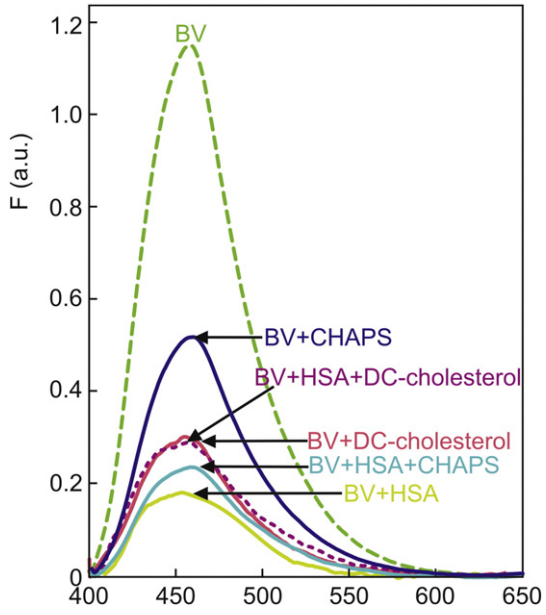

Fig. 7. The fluorescence emission spectra of BV alone in the solution of a phosphate buffer and of BV in the presence of HSA, the DC-cholesterol liposomes, and the CHAPS micelles and in the ternary systems with HSA and the DC-cholesterol liposomes or the CHAPS micelles. The concentration of BV and HSA was 1×10^{-5} M, that of the lipid was 1×10^{-3} M and that of the CHAPS surfactant was 8×10^{-3} M.

more with the polar part of the CHAPS molecules, which is localized on the surface of the micelles. This was implied in the fluorescence spectra (Fig. 7) by the BV with CHAPS micelle band localized at higher wavelength position than the band of the BV with HSA solution. In the solutions of the unordered surfactant, BV probably interacted with the whole surfactant molecule.

As was mentioned above, cholesterol, an important part of human cell membranes, has a similar structural unit to CHAPS and DC-cholesterol. We had prepared several types of liposomes from different lipids and cholesterol and the interaction with BV was not observed even at high cholesterol concentrations. This rules out the possibility of BV interaction solely with the inner part of the model membranes and supports the idea of BV interaction with polar groups closer to the model membrane surface.

Similarly to the BR system, we found that both studied systems of model membranes are suitable chiral selectors that preferentially bind one of the BV enantiomers. The same enantiomeric form of BV was selected by both the models. Consequently, the BV interactions with similarly composed membranes in the human organism or with membranes with the same charge, especially in the case of a positive charge, may occur in the human organism. This may lead to cell membrane disturbance particularly because BV penetrated inside the DC-cholesterol liposomes.

3.4. Biliverdin in the presence of membrane selectors and human serum albumin

The importance of the study with serum albumin was shown in the systems with BR, therefore, we carried out a similar study with BV as well. Fig. 8A depicts the ECD spectra of BV with HSA, for the pigment:HSA ratios from 1:1 to 5:1. In the presence of HSA, BV had an ECD signal consisting of a negative band at 680 nm and a positive band at 382 nm. The spectral intensity was similar only for the 1:1 and 2:1 BV:HSA ratios. The increasing ratio did not cause any changes in the region of HSA absorption which only moderately overlapped the region of BV absorption. In the UV–vis absorption spectral series, several differences were observed between the spectrum of BV and the spectrum of BV with HSA for the 1:1 ratio. The higher-wavelength absorption band shifted from 671 to 667 nm and its intensity increased. On the other hand, the lower-wavelength absorption band shifted from 375 to 380 nm and its intensity decreased. With increasing BV:HSA ratios, no other significant changes were observed. These observations suggest that BV has two binding sites in the structure of HSA, both of them with the M stereoselectivity. The non-proportional change of the intensity of the positive and negative ECD band between the 1:1 and 2:1 BV:HSA ratios indicated that different BV forms of the same chirality bound. The band at 667 nm is particularly sensitive to the BV structure and to the torsion angle between the two parts of the BV molecule. Hence, the smaller increase of its intensity in the ECD spectra proposed that the second binding site bound a different form of M-helical BV. Generally, the difference between the UV–vis spectra of BV alone and with HSA shows that the torsion angle in the bound and unbound BV was different as well.

The interaction of BV with the DC-cholesterol liposomes in the presence of HSA is depicted in Fig. 8B. Remarkably, the spectra differ significantly from the spectral series measured for BV with HSA without model membranes (Fig. 8A). For all the studied ratios, a positive band was observed at 663 nm and a negative band at 408 nm. This spectral pattern indicates the P-form of bound BV which was not observed for the BV binding to HSA. The shape and the position of the positive band were the same as for BV bound to the DC-cholesterol liposomes. The only difference was that the negative band was slightly shifted towards higher wavenumbers. Also, the observed intensities were low and similar to the spectra of BV bound to the liposomes. These all indicate that unlike BR, BV bound dominantly to the DC-cholesterol liposomes even in the presence of HSA. The position and shape of the fluorescence emission spectrum (Fig. 7) were similar to the spectrum of BV bound to the DC-cholesterol liposomes and its analysis showed that only 5% of BV was unbound and of the 95% of bound BV only 6% bound to HSA and 94% to the liposomes (Table S3) for the 1:1 ratio. The UV–vis spectra analysis (Table S2) showed that for the higher ratios more than 95% of bound BV was bound to the liposomes. This interesting fact implies that, although the chemical structure of the two pigments is quite similar, their binding possibilities are very different. While BV preferred unequivocally to bind to the liposomes, BR bound to both the components.

In the study with BSA (Supplementary material), the binding to BSA occurred even to a lesser extent than in the presence of HSA. A slightly smaller effect of the liposomes on the BSA structure than on the HSA structure was observed (Supplementary material, Chapter 1.2, Fig. S3, Tables S2 and 3).

For BV with HSA and CHAPS (Fig. 8C), quite unexpected and unusual spectra of BV were obtained. Their shape was only slightly dependent on the presence of the CHAPS micelles or unordered CHAPS molecules (given by the CMC of CHAPS). A positive band was observed both at higher and lower wavelengths for the 1:1 ratio of BV:HSA. No spectral shifts dependent on the presence of the CHAPS micelles or unordered CHAPS molecules were observed in the UV–vis absorption spectra (Fig. 8C). Although, the two ECD bands commonly observed for BV are not part of a couplet, they usually have opposite signs. The complex pattern observed in our case suggests a very specific binding of BV. The observed spectra for the 1:1 ratio indicate BV binding mainly to HSA but for a different spatial structure of BV than is usual. The fluorescence spectra analysis showed that only 13% of bound BV was bound to the micelles (Table S3).

The slight shift in the absorption maxima for the higher ratios indicated also partial binding to the CHAPS micelles. A small effect of the CHAPS micelles on the tertiary structure of HSA was observed. However, in the region from 200 to 260 nm, where the secondary structure of proteins is reflected, more changes were observed. These changes were evaluated by the CDNN software (developed by Gerald Bohm of University of Halle, Germany [45]). The loss of helicity was suggested to be about 15% (Table S1, Supplementary material, Chapter 2). This could be due to the free CHAPS molecules, because the loss of helicity

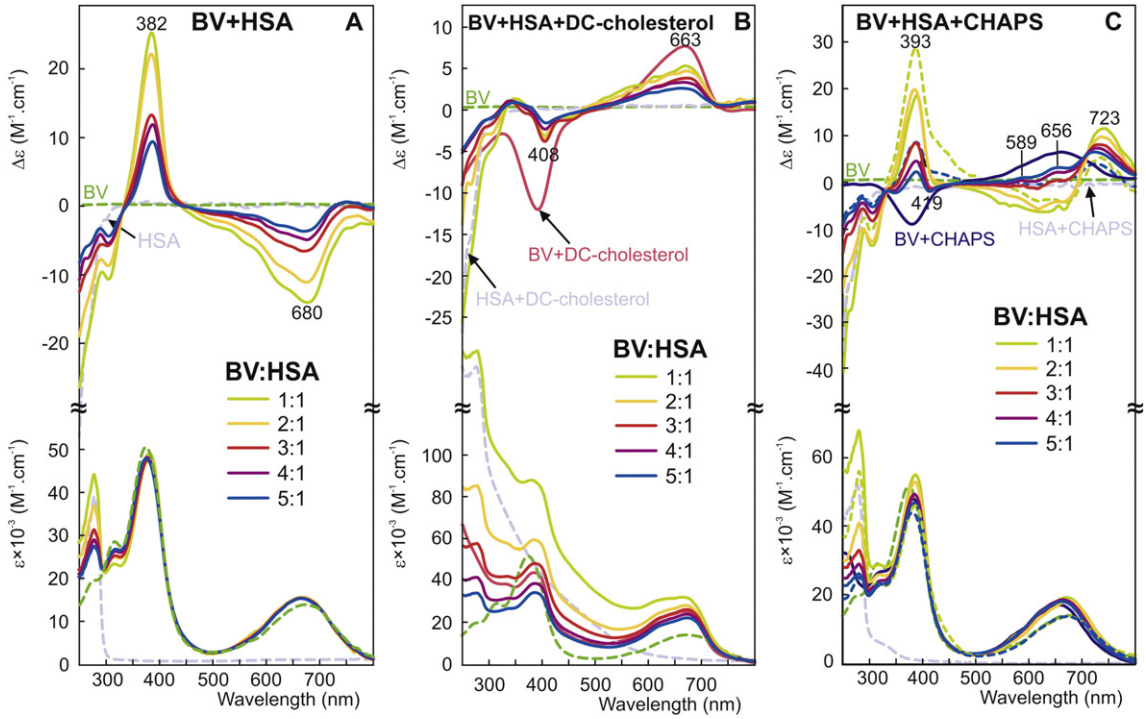

Fig. 8. A: The ECD (top) and UV–vis absorption spectra (bottom) of BV with HSA measured for the BV:HSA ratio from 1:1 to 5:1. The ECD spectra of HSA and BV are also shown. B: The ECD (top) and UV–vis absorption spectra (bottom) of BV with HSA in the presence of the DC-cholesterol liposomes measured for the BV:HSA ratios from 1:1 to 5:1. The ECD spectra of HSA with the DC-cholesterol liposomes, of BV and of BV with the DC-cholesterol liposomes are also shown. C: The ECD (top) and UV–vis absorption spectra (bottom) of BV with HSA in the presence of the CHAPS micelles measured for the BV:HSA ratios from 1:1 to 5:1. The ECD spectra of HSA with the CHAPS micelles, of BV and of BV with the CHAPS micelles are also shown. The spectra measured under CMC are shown as dashed. The concentration of HSA was 1×10^{-5} M, that of the lipid was 1×10^{-3} M, that of the CHAPS was 8×10^{-3} and 2×10^{-3} M and that of BV was given by the BV:HSA ratio and was in the region of 1×10^{-5} M–5×10^{-5} M.

was observed independently of CMC. Nearly no consequences of this were observed for the BR binding to HSA. Nevertheless, the binding sites of BR and BV are localized at different places of the HSA structure. CHAPS probably influenced only the BV binding site and, as the spectra suggest, both BV and CHAPS bound together and this caused changes in the torsion angle between the BV chromophores.

The CHAPS influence on the BV binding sites in the structure of serum albumin was also observed in the study with BSA (Supplementary material, Chapter 1.2, Fig. S3, Tables S2 and 3). In this case, CHAPS even caused that more of the BV molecules bound to BSA than what was observed in the binary system of BV and BSA. The binding to the CHAPS micelles was only very moderate.

In contrast to BR, BV significantly preferred to bind to the DC-cholesterol liposomes over the HSA and BSA. This was probably caused by several factors: a slightly lower binding constant to HSA than that of BR and the double bond in the central part of the BV molecule changing the polarity of the pigment and making its structure more rigid with the polar groups closer together. This more packed structure with exposed polar parts might have also caused the localization of the BV molecule more inside of the bilayer of the DC-cholesterol liposomes than BR. Hence, we suppose that even in the presence of HSA, BV would probably significantly prefer to bind to positively charged domains in human cell membranes and consequently cause disruptions in membrane structures as it is not a desirable component for them.

The remarkable observation made in the BV system with the CHAPS micelles documents the difference between the BR and BV pigments which are constantly compared. Unlike the BR system, the CHAPS molecules probably bound to the similar site of serum albumin as BV and, hence, radically changed the BV binding mechanism. This is analogical to the states that may occur in human organism when one of the pigment binding sites in the structure of HSA is blocked by a drug or other different compounds.

4. Conclusions

Our results implied that both our liposomal model from DC-cholesterol and our micellar model from CHAPS can serve as interesting enantioselective selectors of BR and BV. While the DC-cholesterol liposomes recognized the P-form of BR, the CHAPS micelles recognized its M-form. Both types of model membranes recognized the P-form of BV but the corresponding spectral patterns were a bit different. Also the different nature of the BR and BV interactions influenced their possible penetration into the bilayer. Although the micelles and especially the liposomes do not represent a simple selector model, they provide good enantioselective qualities and not a very strong bond with the bile pigments which might be useful in some studies or applications.

We showed that the BR and BV pigments have more differences in their behavior and interactions than is usually presumed. We found that BR binding to positively charged membranes is less probable in the presence of serum albumin as compared to BV. BV binds to different sites of the protein than BR and therefore is more prone to bind to the positively charged membranes. This indicates its higher toxicity towards such cell membranes in living organisms. The remarkable observation made in the BV system with the CHAPS micelles documents the difference between the two pigments.

Acknowledgment

Financial support from Specific University Research MSMT No 20/2013 (A2_FCHI_2013_010) and MSMT No 20/2015 (A1_FCHI_2015_003) and by the Czech Science Foundation (P206/11/0836, P208/11/0105) is gratefully acknowledged. It was also supported by "Operational Program Prague — Competitiveness" (CZ.2.16/3.1.00/22197) and the "National Program of Sustainability" (NPU) MSMT — LO1215; 34807/2013).

Appendix A. Supplementary data

Supplementary data to this article can be found online at http://dx.doi.org/10.1016/j.bpc.2015.06.001.

References

[1] S. Gazzin, N. Strazielle, C. Tiribelli, J.-F. Ghersi-Egea, Transport and metabolism at blood–brain interfaces and in neural cells: relevance to bilirubin-induced encephalopathy, Front. Pharmacol. 3 (2012) 1–13.
[2] A.F. McDonagh, Turning green to gold, Nat. Struct. Biol. 8 (2001) 198–200.
[3] S.E. Boiadjiev, D.A. Lightner, Optical activity and stereochemistry of linear oligopyrroles and bile pigments, Tetrahedron Asymmetry 10 (1999) 607–655.
[4] H. Falk, T. Schlederer, Beiträge zur Chemie der Pyrrolpigmente, XXX. Struktur und Eigenschaften der Laktimform eines Bilatriens-abc (ätiobiliverdin-IV-γ), Liebigs Ann. Chem. 1979 (1979) 1560–1570.
[5] M. Zahedi, N. Safari, S. Haddadpour, Semiempirical molecular orbital calculations of biliverdin: study of dynamics and energetics of the self-association of a two-electron oxidation product, J. Mol. Struct. THEOCHEM 531 (2000) 79–88.
[6] M. Zahedi, A. Shaabani, N. Safari, Semiempirical molecular orbital calculations of biliverdin: stability study of various isomers and conformation analysis, J. Mol. Struct. THEOCHEM 452 (1998) 125–131.
[7] I. Goncharova, S. Orlov, M. Urbanova, Chiroptical properties of bilirubin–serum albumin binding sites, Chirality 25 (2013) 257–263.
[8] I. Goncharova, M. Urbanova, Bile pigment complexes with cyclodextrins: electronic and vibrational circular dichroism study, Tetrahedron Asymmetry 18 (2007) 2061–2068.
[9] I. Goncharova, M. Urbanová, Vibrational and electronic circular dichroism study of bile pigments: complexes of bilirubin and biliverdin with metals, Anal. Biochem. 392 (2009) 28–36.
[10] O. Julínek, I. Goncharova, M. Urbanová, Chiral memory and self-replication study of porphyrin and bilirubin aggregates formed on polypeptide matrices, Supramol. Chem. 20 (2008) 643–650.
[11] D.A. Lightner, M. Reisinger, G.L. Landen, On the structure of albumin-bound bilirubin. Selective binding of intramolecularly hydrogen-bonded conformational enantiomers, J. Biol. Chem. 261 (1986) 6034–6038.
[12] M. Reisinger, D.A. Lightner, Bilirubin conformational enantiomer selection in sodium deoxycholate chiral micelles, J. Incl. Phenom. 3 (1985) 479–485.
[13] K. Kano, Mechanisms for chiral recognition by cyclodextrins, J. Phys. Org. Chem. 10 (1997) 286–291.
[14] K. Kano, S. Arimoto, T. Ishimura, Conformational enantiomerism of bilirubin and pamoic acid induced by protonated aminocyclodextrins, J. Chem. Soc. Perkin Trans. 2 (1995) 1661–1666.
[15] K. Kano, K. Imaeda, K. Ota, R. Doi, Reexamination of cyclodextrin-induced conformational enantiomerism of bilirubin in aqueous solution, Bull. Chem. Soc. Jpn. 76 (2003) 1035–1041.
[16] D.A. Lightner, J.K. Gawroński, K. Gawrońska, Conformational enantiomerism in bilirubin. Selection by cyclodextrins, J. Am. Chem. Soc. 107 (1985) 2456–2461.
[17] I. Goncharova, S. Orlov, M. Urbanova, The location of the high- and low-affinity bilirubin-binding sites on serum albumin: ligand-competition analysis investigated by circular dichroism, Biophys. Chem. 180 (2013) 55–65.
[18] J. Jacobsen, R. Brodersen, Albumin–bilirubin binding mechanism. Kinetic and spectroscopic studies of binding of bilirubin and xanthobilirubic acid to human serum albumin, J. Biol. Chem. 258 (1983) 6319–6326.
[19] A. Knudsen, A.O. Pedersen, R. Brodersen, Spectroscopic properties of bilirubin–human serum albumin complexes: a stoichiometric analysis, Arch. Biochem. Biophys. 244 (1986) 273–284.
[20] R.A. Weisiger, J.D. Ostrow, R.K. Koehler, C.C. Webster, P. Mukerjee, L. Pascolo, C. Tiribelli, Affinity of human serum albumin for bilirubin varies with albumin concentration and buffer composition: results of a novel ultrafiltration method, J. Biol. Chem. 276 (2001) 29953–29960.
[21] P. Novotna, I. Goncharova, M. Urbanova, Mutual structural effect of bilirubin and model membranes by vibrational circular dichroism, Biochim. Biophys. Acta Biomembr. 1838 (2014) 831–841.
[22] D.A. Lightner, J.K. Gawronski, W.M.D. Wijekoon, Complementarity and chiral recognition: enantioselective complexation of bilirubin, J. Am. Chem. Soc. 109 (1987) 6354–6362.
[23] J. Novotná, I. Goncharova, M. Urbanová, Guanosine assemblies: newly used matrices for chiroptical studies on biliverdin, Supramol. Chem. 26 (2014) 7–14.
[24] C. Bernardini, P. D'Arrigo, G. Elemento, G. Mancini, S. Servi, A. Sorrenti, The posssible role of enantiodiscrimination in bilirubin toxicity, Chirality 21 (2009) 87–91.
[25] S. Borocci, F. Ceccacci, O. Cruciani, G. Mancini, A. Sorrenti, Chiral recognition in biomembrane models: what is behind a 'simple model', Synlett (2009) 1023–1033.
[26] D. Brites, The evolving landscape of neurotoxicity by unconjugated bilirubin: role of glial cells and inflammation, Front. Pharmacol. 3 (2012) 88.
[27] M.A. Brito, C.D. Brondino, J.J.G. Moura, D. Brites, Effects of bilirubin molecular species on membrane dynamic properties of human erythrocyte membranes: a spin label electron paramagnetic resonance spectroscopy study, Arch. Biochem. Biophys. 387 (2001) 57–65.
[28] M.A. Brito, R. Silva, C. Tiribelli, D. Brites, Assessment of bilirubin toxicity to erythrocytes. Implication in neonatal jaundice management, Eur. J. Clin. Investig. 30 (2000) 239–247.
[29] A. Sorrenti, B. Altieri, F. Ceccacci, P. Profio, R. Germani, L. Giansanti, G. Savelli, G. Mancini, Deracemization of bilirubin as the marker of the chirality of micellar aggregates, Chirality 24 (2012) 78–85.
[30] C. Bombelli, C. Bernardini, G. Elemento, G. Mancini, A. Sorrenti, C. Villani, Concentration as the switch for chiral recognition in biomembrane models, J. Am. Chem. Soc. 130 (2008) 2732–2733.
[31] D. Voet, J.G. Voet, Biochemistry, Wiley, New York, 2004.
[32] C.B. Berde, B.S. Hudson, R.D. Simoni, L.A. Sklar, Human serum albumin. Spectroscopic studies of binding and proximity relationships for fatty acids and bilirubin, J. Biol. Chem. 254 (1979) 391–400.
[33] S. Curry, P. Brick, N.P. Franks, Fatty acid binding to human serum albumin: new insights from crystallographic studies, Biochim. Biophys. Acta Mol. Cell Biol. Lipids 1441 (1999) 131–140.
[34] A. Sri Ranjini, P.K. Das, P. Balaram, Binding constant measurement by hyper-Rayleigh scattering: bilirubin–human serum albumin binding as a case study, J. Phys. Chem. B 109 (2005) 5950–5953.
[35] J. Claret, O. Ibars, K. Lang, F.R. Trull, D.A. Lightner, Electrochemical reduction of the biliverdin–serum albumin complex as monitored by absorption and circular dichroism spectroscopy, Biochim. Biophys. Acta Gen. Subj. 1243 (1995) 221–229.
[36] F.R. Trull, O. Ibars, D.A. Lightner, Conformation inversion of bilirubin formed by reduction of the biliverdin–human serum albumin complex: evidence from circular dichroism, Arch. Biochem. Biophys. 298 (1992) 710–714.
[37] G. Blauer, G. Wagniere, Conformation of bilirubin and biliverdin in their complexes with serum-albumin, J. Am. Chem. Soc. 97 (1975) 1949–1954.
[38] V.P. Torchilin, V. Weissig, Liposomes: A Practical Approach, Oxford University Press, New York, 2003. 3–8.
[39] P. Novotna, M. Urbanova, Vibrational circular dichroism study of polypeptide model-membrane systems, Anal. Biochem. 427 (2012) 211–218.
[40] A.L. Russell, A.M. Kennedy, A.M. Spuches, D. Venugopal, J.B. Bhonsle, R.P. Hicks, Spectroscopic and thermodynamic evidence for antimicrobial peptide membrane selectivity, Chem. Phys. Lipids 163 (2010) 488–497.
[41] S.Y. Wen, M. Majerowicz, A. Waring, F. Bringezu, Dicynthaurin (ala) monomer interaction with phospholipid bilayers studied by fluorescence leakage and isothermal titration calorimetry, J. Phys. Chem. B 111 (2007) 6280–6287.
[42] T. Wieprecht, O. Apostolov, M. Beyermann, J. Seelig, Membrane binding and pore formation of the antibacterial peptide PGLa: thermodynamic and mechanistic aspects, Biochemistry 39 (2000) 442–452.
[43] T. Wieprecht, O. Apostolov, J. Seelig, Binding of the antibacterial peptide magainin 2 amide to small and large unilamellar vesicles, Biophys. Chem. 85 (2000) 187–198.
[44] T. Wieprecht, M. Beyermann, J. Seelig, Thermodynamics of the coil–alpha-helix transition of amphipathic peptides in a membrane environment: the role of vesicle curvature, Biophys. Chem. 96 (2002) 191–201.
[45] G. Bohm, R. Muhr, R. Jaenicke, Quantitative-analysis of protein far UV circular-dichroism spectra by neural networks, Protein Eng. 5 (1992) 191–195.
[46] J.R. Lakowicz, Principles of Fluorescence Spectroscopy, Springer, 2007.
[47] U. Neugebauer, A. März, T. Henkel, M. Schmitt, J. Popp, Spectroscopic detection and quantification of heme and heme degradation products, Anal. Bioanal. Chem. 404 (2012) 2819–2829.
[48] W.E. Kurtin, J. Enz, C. Dunsmoor, N. Evans, D.A. Lightner, Acid dissociation constants of bilirubin and related carboxylic acid compounds in bile salt solutions, Arch. Biochem. Biophys. 381 (2000) 83–91.
[49] D.A. Lightner, D.L. Holmes, A.F. McDonagh, On the acid dissociation constants of bilirubin and biliverdin: pK_a values from ^{13}C NMR spectroscopy, J. Biol. Chem. 271 (1996) 2397–2405.
[50] F.R. Trull, S. Boiadjiev, D.A. Lightner, A.F. McDonagh, Aqueous dissociation constants of bile pigments and sparingly soluble carboxylic acids by 13C NMR in aqueous dimethyl sulfoxide: effects of hydrogen bonding, J. Lipid Res. 38 (1997) 1178–1188.
[51] P. Novotná, M. Urbanová, Bilirubin, model membranes and serum albumin interaction: the influence of fatty acids, Biochim. Biophys. Acta Biomembr. 1848 (2015) 1331–1340.